Multi-drug-resistance efflux in cisplatin-naive and cisplatin-exposed A2780 ovarian cancer cells responds differently to cell culture dimensionality

VASILIJ KOSHKIN[1], MARIANA BLEKER DE OLIVEIRA[1], CHUN PENG[1], LAURIE E. AILLES[2], GEOFFREY LIU[3], ALLAN COVENS[4] and SERGEY N. KRYLOV[1]

[1]Centre for Research on Biomolecular Interactions, York University, Toronto, Ontario M3J 1P3; [2]Department of Medical Biophysics, University of Toronto, Toronto, Ontario M5G 1L7; [3]Department of Medicine, Medical Oncology, Princess Margaret Cancer Centre, Toronto, Ontario M5G 2M9; [4]Sunnybrook Odette Cancer Centre, Toronto, Ontario M4N 3M5, Canada

Received January 20, 2021; Accepted June 2, 2021

DOI: 10.3892/mco.2021.2323

Abstract. A primary reason for chemotherapy failure is chemoresistance, which is driven by various mechanisms. Multi-drug resistance (MDR) is one such mechanism that is responsible for drug extrusion from the intracellular space. MDR can be intrinsic and thus, may pre-exist the first application of chemotherapy. However, MDR may also be acquired during tumor exposure to chemotherapeutic agents. To understand whether cell clustering can influence intrinsic and acquired MDR, the present study assessed cultured monolayers (representing individual cells) and spheroids (representing clusters) formed by cisplatin-naïve (intrinsic MDR) and cisplatin-exposed (acquired MDR) lines of ovarian cancer A2780 cells by determining the cytometry of reaction rate constant (CRRC). MDR efflux was characterized using accurate and robust cell number vs. MDR efflux rate constant (k_{MDR}) histograms. Both cisplatin-naïve and cisplatin-exposed monolayer cells presented unimodal histograms; the histogram of cisplatin-exposed cells was shifted towards a higher k_{MDR} value suggesting greater MDR activity. Spheroids of cisplatin-naïve cells presented a bimodal histogram indicating the presence of two subpopulations with different MDR activity. In contrast, spheroids of cisplatin-exposed cells presented a unimodal histogram qualitatively similar to that of the monolayers of cisplatin-exposed cells but with a moderate shift towards greater MDR activity. A flow-cytometry assessment of multidrug resistance-associated protein 1 transporter levels in monolayers and dissociated spheroids revealed distributions similar to those of k_{MDR}, thus, suggesting a plausible molecular mechanism for the observed differences in MDR activity. The observed greater effect of cell clustering on intrinsic rather than in acquired MDR can help guide the development of new therapeutic strategies targeting clusters of circulating tumor cells.

Correspondence to: Professor Sergey N. Krylov, Centre for Research on Biomolecular Interactions, York University, Petrie Science Building, Room 343, Toronto, Ontario M3J 1P3, Canada
E-mail: skrylov@yorku.ca

Abbreviations: ABC, ATP-binding cassette; CRRC, cytometry of reaction rate constant; CTC, circulating tumor cells; MDR, multi-drug resistance; OC, ovarian cancer

Key words: intrinsic multi-drug resistance, acquired multi-drug resistance, circulating tumor cells, single cells, cell clusters, cell monolayer, multi-cellular spheroids, cytometry of reaction rate constant, ovarian cancer

Introduction

Chemoresistance (intrinsic and acquired) is the main reason for cancer chemotherapy failure and patients' death in the Western world (1). There are several cellular processes that contribute to both intrinsic and acquired chemoresistance (2). One of such processes is active extrusion of drugs from cells by ATP-binding cassette transporters (ABC transporters), which are membrane proteins (3). This process has low drug specificity and is termed multi-drug resistance (MDR). Here, we use the term MDR solely to describe the catalytic process of drug transport across the membrane (from inside to outside of the cell). Activity of MDR in tumor cells has been shown to correlate with clinical chemoresistance, and MDR is its likely driver (4).

A promising approach in cancer research is studying circulating tumor cells (CTCs). CTCs exist as individual cells or multicellular clusters that detach from the primary tumor, circulate in the bloodstream, and give rise to systemic metastases and tumor relapse (5). CTC clusters are reported to be more chemoresistant than individual CTCs (6), and the density of CTC clusters in blood was found to correlate with clinical features of cancer (7).

The presumed roles of MDR transport and CTC clusters in the development of chemoresistance logically lead to a question: Can cell clustering influence intrinsic and acquired MDR differently? To the best of our knowledge, this question

has never been addressed. Addressing this question requires a cytometry technique capable of accurately measuring MDR activity and applicable to both single cells and intact clusters. Classical cytometry techniques cannot be used for accurate measurements of MDR activity, making the above-posed question difficult to approach experimentally. In contrast, cytometry of reaction rate constant (CRRC) can be used for this purpose. CRRC utilizes time-lapse fluorescence microscopy to measure a rate constant of a catalytic reaction in individual cells, thus, facilitating accurate frequency determination for subpopulations of cells with distinct activities of this reaction (8). Time-lapse fluorescence images are used to build kinetic traces of substrate conversion into a product. A reaction rate constant is then found for every cell using a known mechanism of the reaction. Finally, a CRRC histogram, which plots the number of cells versus the rate constant value, is used to accurately measure frequencies of cell subpopulations with distinct reaction activities (8).

When applied to MDR transport, CRRC is used to record kinetics of fluorescent substrate extrusion from cells (Fig. 1). The extrusion process is governed by the Michalis-Menten mechanism, which is characterized by two parameters: The maximum velocity, V_{max}, and the Michaelis constant, K_M. A ratio between these parameters is a first order rate constant of MDR transport, $k_{MDR}=V_{max}/K_M$, which can be easily determined from time dependence of intracellular fluorescence intensity of an MDR substrate. CRRC histograms that plot the number of cells vs. k_{MDR} ranges are robust towards variations in substrate concentration and observation time (8); therefore, such histograms facilitate accurate determining the sizes of cell subpopulations with different MDR activities (8).

The most straightforward application of CRRC is in 2D models, such as cells cultured as monolayers or cells obtained by disintegration of cell clusters (e.g. spheroids or tissue samples) and allowed to settle on a surface (9). However, if CRRC is based on confocal microscopy, it can also be applied to 3D models, i.e., intact cell clusters and spheroids in particular (9). Specific features of CRRC-based MDR studies in spheroids are described in detail elsewhere (9). Two important remarks should be made at this point. First, due to its transmembrane nature, the MDR process should be studied in small spheroids of ~100 μm in diameter. Small spheroids facilitate free MDR efflux from approximately 70% of spheroid cells and also minimize intraspheroidal gradients of oxygen, pH, etc. (9,10). Second, since the first order rate constant is defined by the dynamics rather than the absolute values of fluorescence signal, the CRRC method is robust to variations in substrate level or signal attenuation potentially associated with cell clustering or uneven illumination.

Thus, CRRC is uniquely capable of accurately measuring MDR activity in both 2 and 3D models, making it suitable for addressing our question of how MDR activity of single cells differs from that of aggregated cells in i) drug-naïve and ii) drug-exposed tumor cells. In this study, drug-naïve and drug-exposed tumor cells were modeled by the parental and cisplatin-resistant variants of the A2780 ovarian cancer (OC) cell line (A2780S and A2780CP, respectively) (11,12). Analytical advantages of A2780 cells include their inducible MDR capacity (13), ability to form small compact spheroids (14), and extensive use in the development of CRRC (8,9). From the clinical point of view, OC is especially prone to chemoresistance (15), and these cells are viewed as an appropriate general model of OC, though not for its common high-grade serous form (16). In addition, A2780 cells were previously used to mimic ovarian CTCs (17).

The A2780S cell subline is derived from a patient who was not exposed to chemotherapy, and, thus, this cisplatin-naïve cell line represents intrinsic chemoresistance (18). The A2780CP cell subline is derived from the A2780S subline and has been cultured in the presence of cisplatin to develop resistance to this drug. Therefore, A2780CP cells represent OC cells that have developed acquired chemoresistance in response to cisplatin, a standard chemotherapeutic agent for first-line OC treatment. Importantly, both cell lines can be grown as monolayers or as multicellular spheroids (14). Therefore, we can view cultured monolayers of A2780S and A2780CP cells as models of circulating single cells, while their cultured spheroids can be considered as models of CTC clusters. Comparison of CRRC histograms of a cell monolayer with that of cultured spheroids can then answer our question. It is important to emphasize that our study is limited to one cell line and one drug; answering our question for other cell lines (and drugs) will require further investigation.

Materials and methods

CRRC experimental techniques. Detailed description of experimental techniques of CRRC for cell monolayers and cells in intact spheroids, as well as cell source, can be found elsewhere (9); these techniques were followed exactly with no modification of the procedures.

Cell cultures. A2780S and A2780CP cell lines are per se sublines of A2780 cells which can be cultured in the same way. Briefly, the cells were cultured as monolayers at 37˚C in a humidified atmosphere of 5% CO_2, in Dulbecco's modified Eagle's medium (DMEM, containing 4.5 g/l glucose, 1.5 g/l sodium bicarbonate, 1 mM sodium pyruvate, and 4 mM L-glutamine) and supplemented with fetal bovine serum [10% (vol/vol)], penicillin (100 IU) and streptomycin (100 μg/ml). Medium was produced by the American Type Culture Collection (ATCC, ATCC30-2002) and was obtained from Cedarlane. The medium was replaced by fresh medium every 2 days. The culturing of small multicellular spheroids was based on the liquid overlay approach (19) adapted for ovarian cells (20). Briefly, 96-well plates were treated with 100 μl of 10% agarose per well to create a concave non-adhesive surface. After the solidification of agarose, the wells were filled with 100 μl of cell suspension ($5x10^3$ cells/ml) in DMEM, and spheroids were allowed to form for 2-3 days before their collection. For time-lapse imaging, spheroids were placed onto coverslips and allowed to settle and attach to the surface for 5 h (21).

Imaging. The imaging of MDR efflux was performed with a FV300 confocal cell imager (Olympus) in the time-lapse mode for 120 min with single and multiple optical sections taken for monolayers and spheroids, respectively. Cells were loaded with a fluorescent MDR substrate (fluorescein) and allowed to extrude it. The kinetics of substrate extrusion was monitored

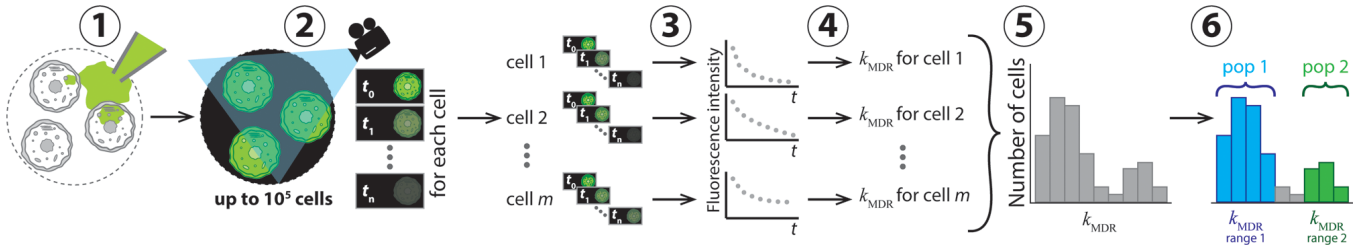

Figure 1. Conceptual representation of application of CRRC to MDR in six consecutive steps. In step 1, the cells were loaded with a fluorescent substrate of ABC transporters which was then removed from the cell media to initiate substrate extrusion. In step 2, the kinetics of decreasing fluorescence intensity was measured microscopically. Sequential images of the individual cells were taken at various times over a period of time exceeding the characteristic time of the extrusion reaction. In step 3, kinetic traces of fluorescence intensity for every cell were constructed. In step 4, values of the reaction rate constant, k_{MDR}, were determined for each cell. In step 5, these values were used to build a CRRC histogram with the number of cells vs. k_{MDR}. In step 6, the heterogeneity of cell population with respect to MDR activity was characterized accurately using the histogram: Cell subpopulations with different MDR activities were identified and quantified. CRRC, cytometry of reaction rate constant; MDR, multi-drug resistance; pop, subpopulation; t, time; *m*, cell number in a cell population (1, 2, *m*).

by measuring intracellular fluorescence intensity over time to determine k_{MDR} for individual cells. To avoid the underestimation of MDR efflux due the MDR probe accumulation in the intercellular space, only outer spheroidal cells were taken into consideration. The small diameter of the spheroids used in this study (~100 μm) ensured that the outer cells constituted ~70% of the spheroid cell population. This minimized the intra-spheroid oxygen gradient and, thus, hypoxia with its potential effect on MDR. It was shown previously that the outer cells in such spheroids well represented the entire spheroidal cell population (9).

CRRC histograms. Kinetic cytometry histograms were plotted and peak maximum positions in these histograms were determined for the comparison of MDR activity (k_{MDR}) in the monolayers and spheroids of A2780S and A2780CP cell lines.

Multidrug resistance-associated protein 1 (MRP1) expression assay. Expression levels of the MRP1 transporter in monolayers and dissociated spheroid cells were estimated using flow cytometry with FITC-labeled mouse anti-human MRP1 antibody QCRL-3 and an isotype control (FITC Mouse IgG2a) (BD Biosciences, cat. no. 557593 and 555573, respectively) according to the previously published procedure (22). Briefly, monolayers and spheroids were trypsinized with 0.25% trypsin/0.02% EDTA to form single cell suspensions, permeabilized with 80 μg/ml saponin, treated with the antibodies, and analyzed with a BD FACSCanto II flow cytometer.

Statistical analysis. Differences between cells in regards to basal transporter activity and expression (A2780S monolayer cells) and other cell types were analyzed for statistical significance using one-way ANOVA followed by the Dunnett test, using Origin software (version 9.4, OriginLab). Data are presented as mean ± SE, n=3, $P<0.05$ was determined to indicate a statistically significant difference.

Results

Time-lapse imaging. We grew cultured A2780S and A2780CP cells as monolayers and spheroids, loaded them with fluorescein (a fluorescent substrate of ABC transporters) and imaged fluorescein extrusion from the cells with confocal laser-scanning microscopy as described in Materials and Methods. A standard end-point analysis, which is commonly used in MDR studies, compares fluorescence of cells at two time points: Immediately after loading them with the fluorescent substrate and 2 h later (8,23,24). Representative images in the top and bottom in Fig. 2 show a similar ability of all cell types for nearly complete extrusion of MDR probe after 2 h. However, images taken in the middle of this 2-h period (Fig. 2, middle row) suggest that A2780S monolayer cells may extrude the substrate more slowly than A2780S spheroid cells, as well as both types of A2780CP cells.

Kinetic analysis. The end-point analysis of the images does not allow one to make any further conclusion; therefore, MDR activity was elicited from the CRRC kinetic analysis. We processed images from 347 cells in each of the four categories (cisplatin-naïve single cells, cisplatin-naïve spheroidal cells, cisplatin-exposed single cells, and cisplatin-exposed spheroidal cells) to determine k_{MDR} for each cell and plot CRRC histograms (Fig. 3).

CRRC histograms of the cisplatin-naïve A2780S cell line are shown in Fig. 3A and summarized in Table I; they have been adopted from our recently published paper (9). The monolayer histogram (grey line) was found to be unimodal, suggesting a single population of cells. The spheroid histogram (black line) revealed a bimodal distribution, suggesting two cell subpopulations: The first one is larger and has the same peak k_{MDR} value as the monolayer cells, while the second one is smaller and has a peak k_{MDR} value which is almost 3 times greater. This latter subpopulation has a greater MDR capacity, and its appearance is caused by cell-cell interactions in the 3D spheroids (25). The presence of a cisplatin-resistant subpopulation (presumably containing tumor initiating cells) in the spheroids is consistent with the notion that CTC clusters have a greater drug-resistance capacity than single CTCs. The unimodal right-skewed histogram of monolayer A2780S cells is similar to that reported earlier (8). Its shape is consistent with the often reported asymmetric expression of MDR transporters, when the majority of cells with a basal (low) level of transporter expression form the main peak and a much smaller subpopulation of cells with elevated transporter expression forms the distribution tail towards higher k_{MDR} values (26).

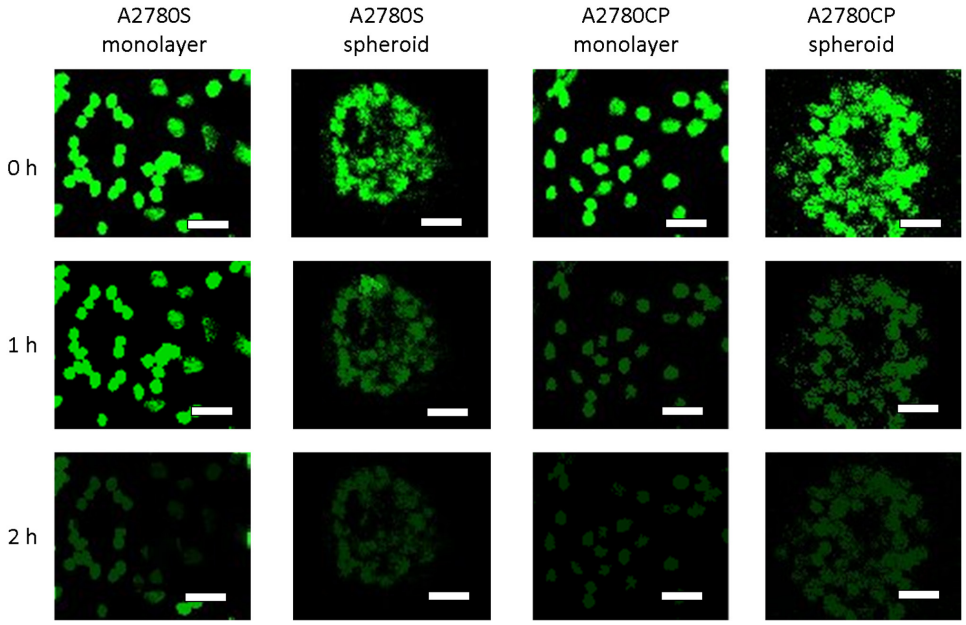

Figure 2. Representative images of monolayer-grown cells and spheroid-grown cells for the cisplatin-naïve A2780S cell line and its derivative cisplatin-exposed A2780CP cell line. The top, middle and bottom images were obtained at 0, 1 and 2 h after the beginning of fluorescein extrusion (scale bar, 30 μm).

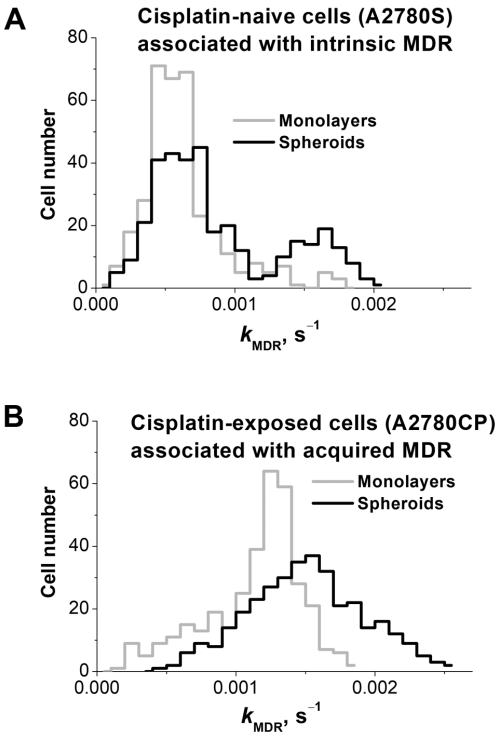

Figure 3. Cytometry of reaction rate constant histograms of cell subpopulation frequencies determined using MDR transport first order rate constant (k_{MDR}, measured in s^{-1}) in monolayer-grown (grey lines) and spheroid-grown (black lines) (A) cisplatin-naïve A2780S cells and (B) derivative cisplatin-exposed A2780CP cells. Traces in panel (A) have been reproduced from Fig. 4 in reference (9) with permission from the American Chemical Society. MDR, multi-drug resistance.

When A2780S cells are cultured as spheroids, the tail becomes a distinct peak, which corresponds to a distinct subpopulation of cells with its own elevated peak k_{MDR} value: The histogram becomes bimodal. This bimodality is not associated with cell position in the 3D spheroids as only the outer spheroidal cells were analyzed. It is remarkable that the activation of MDR transport in spheroidal A2780S cells is not distributed equally across all spheroidal cells. Instead, the activation proceeds through increasing the size of the subpopulation of cells with a greater MDR-transport activity. This characteristic of MDR modulation agrees well with the notion that the size and activity of the drug-resistant subpopulation determine the overall resistance of a heterogeneous cell population (27).

CRRC histograms of the cisplatin-exposed (drug-resistant) A2780CP cell line are depicted in Fig. 3B and summarized in Table I. Monolayer cells (grey line) showed a unimodal distribution with the median (peak) k_{MRD} value exceeding that of monolayer A2780S cells (grey line in Fig. 3A) approximately by a factor of 2. When cultured as spheroids, A2780CP cells also showed a unimodal distribution (black line), and the histogram of the spheroidal A2780CP cells was moderately shifted to the right with respect to that of the monolayer A2780CP cells. In addition, the peak maximum of the spheroidal A2780CP cells was at the same k_{MDR} position as the peak maximum of the drug-resistant subpopulation in the spheroidal A2780S cells (right-hand-side peak in the black line in Fig. 3A). Thus, the drug-resistant subpopulation dominates even in monolayers formed by these cells and predictably dominates in spheroids resulting in a unimodal k_{MDR} distribution in the spheroid culture. The peak maximum value in the spheroid culture slightly exceeds that in the monolayer (by a factor of 1.2). Lower kurtosis (indicator of distribution peakedness/flatness, -0.95 vs. 1.87) indicates that MDR distribution in A2780CP spheroids is more heterogeneous than in monolayers. Greater heterogeneity can be associated with the larger fraction of cells with elevated k_{MDR} able to survive chemotherapy and initiate tumor relapse.

Table I. Peak positions cytometry of reaction rate constant histograms of cisplatin-naïve and cisplatin-exposed monolayer and spheroid cells.

	A2780S cells		A2780CP cells	
Parameter	Monolayer	Spheroid	Monolayer	Spheroid
Positions of peak maximum (s^{-1})	0.00058±0.00008	Left-hand-side peak, 0.00057±0.00009; Right-hand-side peak, 0.00166±0.00019[a]	0.00125±0.00015[a]	0.00164±0.00021[a]

[a]Statistical significance (at P<0.05) of the deviation of each peak maximum position from the basal level of A2780S peak (n=3).

Flow-cytometry study of transporter expression. It is interesting to learn what drives the observed differences in k_{MDR} values in the 2 and 3D cell cultures between the A2780S and A2780CP cells. The MDR transport reaction, characterized by k_{MDR}, translocates the intracellular substrates (S_{in}) across the membrane adding it to the pool of the substrate outside the cell (S_{out}). The reaction proceeds through the formation of an intermediate complex (TS) between the transporter (T) and substrate (S):

$$T + S_{in} \underset{k_{-1}}{\overset{k_1}{\rightleftarrows}} TS \xrightarrow{k_{cat}} T + S_{out} \quad (1)$$

where k_1 is a bimolecular rate constant of TS formation while k_{-1} and k_{cat} are monomolecular rate constants of complex dissociation backwards to S_{in} and forward to S_{out}, respectively. The values of k_1, k_{-1}, and k_{cat} depend on the transporter's microenvironment within the membrane. The pseudo-first order rate constant k_{MDR} used in our study is defined as:

$$k_{MDR} = k_{cat}[T]/K_M \quad (2)$$

where [T] is the transporter concentration, and $K_M=(k_{cat}+k_{-1})/k_1$ is the Michaelis constant, which, accordingly, depends on transporter's microenvironment and is indicative of complex stability. It is clear from equation 2 that k_{MDR} can be influenced either by the expression level of the transporter [(T)] or by transporter microenvironment (k_{cat}/K_M). So, the observed differences in k_{MDR} values in the 2 and 3D cell cultures between A2780S and A2780CP cells can be driven either by different levels of transporter expression or by changes in the transporter's microenvironment. MDR efflux in A2780 cells is typically driven by the MRP1 transporter (13,18), which is in line with significant fluorescein-extruding capacity of these cells observed in this and previous studies (8,9). Therefore, we decided to assess MRP1 expression levels in 2 and 3D cultures to examine if the differences in MRP1 expression levels are a cause for the observed differences in the MDR efflux kinetics. There are multiple ways of studying expression of the MRP1 gene, but for our purpose, the most direct and conclusive way is immunostaining of the MRP1 transporter with fluorescently-labeled antibody interrogated by flow cytometry. The results of flow cytometry are frequency histograms conceptually similar to those of CRRC histograms. Therefore, the cell-population heterogeneity revealed from flow cytometry histograms can be directly compared to the heterogeneity obtained from the CRRC histograms to conclude whether or not the differences in k_{MDR} of the 2 and 3D cultures between A2780S and A2780CP cells are caused by the difference in MRP1 expression levels. Thus, we conducted flow-cytometry experiments to study the population heterogeneity of MRP1 levels. The results for the heterogeneity of MRP1 levels in the populations of A2780S and A2780CP cells grown in monolayers and spheroids are shown in Fig. 4 and Table II. These results clearly indicate that cell clustering causes the formation of a subpopulation with increased expression of the MRP1 transporter in A2780S cells, while this transporter is overexpressed in both the monolayer and spheroids in A2780CP cells. Thus, the differences in k_{MDR} between the 2 and 3D cultures A2780S and A2780CP cells are caused by the difference in MRP1 levels.

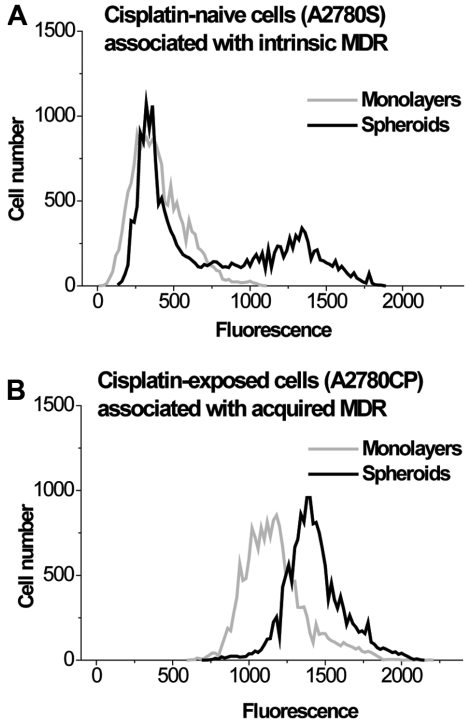

Figure 4. Characteristic profiles of the multidrug resistance-associated protein 1 transporter level in monolayer-grown (gray lines) and spheroid-grown (black lines) (A) cisplatin-naïve A2780S cells and (B) derivative cisplatin-exposed A2780CP cells. MDR, multi-drug resistance.

Table II. Peak positions in flow-cytometry profiles of the expression of multidrug resistance-associated protein 1 in cisplatin-naïve and cisplatin-exposed monolayer and spheroid cells.

	A2780S cells		A2780CP cells	
Parameter	Monolayer	Spheroid	Monolayer	Spheroid
Positions of peak maximum (RFU)	311±29	Left-hand-side peak, 362±42; Right-hand-side peak, 1,298±151[a]	1,171±164[a]	1,403±139[a]

[a]Statistical significance (at P<0.05) of the deviation of each peak maximum position from the basal level of A2780S peak (n=3).

Discussion

Our aim in this study was to determine if cell clustering influences intrinsic and acquired MDR differently. To address this question, we studied cultured monolayers (representing individual cells) and cultured spheroids (representing clusters) formed by cisplatin-naïve (intrinsic MDR) and cisplatin-exposed (acquired MDR) lines of ovarian cancer A2780 cells by CRRC. MDR efflux was characterized by accurate and robust 'cell number vs. MDR efflux rate constant (k_{MDR})' histograms. We observed a greater influence of cell clustering on k_{MDR} distribution in the intrinsic than in the acquired MDR model. The increase of k_{MDR} in the clustered cells can be caused by the increased expression of MDR transporters under 3D conditions. The results of the current study demonstrate agreement, both qualitative and quantitative, between the data for k_{MDR} and MRP1 transporter level. Qualitatively, the bimodal distribution of k_{MDR} in spheroids formed by drug-naïve cells agrees with the bimodal profile of the MRP1 transporter level in these spheroids. Also, the unimodal distributions of k_{MDR} in other cases agree with the unimodal MRP1 level profiles. Quantitatively, both k_{MDR} values and MRP1 levels in the drug-exposed cells exceed those in the drug-naïve cells. The observed overexpression of the MRP1 transporter in spheroids formed by A2780S cells is in line with similar observations made in other cell types (28). In A2780CP cells, the MRP1 level is intrinsically high in the monolayer state and, thus, it responds to cell clustering by only a slight increase. The mechanism of MRP1 overexpression (gene amplification, transcriptional and post-transcriptional regulation) will be addressed in the extended OC spheroid study using RNA-seq and qPCR.

The potential clinical implications of our findings are dual. First, considering the role of clustering of OC cells in intrinsic and acquired chemoresistance, our results provide a new possible explanation for the benefit of debulking surgery that has not yet been theorized; by reducing spheroids and thereby decreasing intrinsic resistance we should improve outcomes. Second, activation of MDR transport within spheroids was ascribed to activation of the HIF pathway caused either by hypoxia inside the spheroids or by cytotoxic agents (29). However, we found MDR-transport activation not only inside the spheroids but also on their surface; moreover, this activation is observed in both drug-naïve (intrinsic MDR) and drug-exposed (acquired MDR) cells. These observations strongly suggest that there are other mechanisms of MDR-transport activation in addition to the HIF-hypoxia pathway. It should be noted that both monolayers and spheroids were in identical cell media during the CRRC analysis, which univocally assigns the observed differences between the monolayers and spheroids to cell culture dimensionality rather than media-caused differences in metabolic processes.

We would like to elaborate on the potential effect of cell migration on our comparative CRRC study of cell monolayers and spheroids. CRRC of MDR transport requires tracking individual cells through a 2-h time-lapse measurement. This can be achieved only by using a time interval between the frames in the minute scale, which is much shorter than the characteristic time of cell's moving a distance equal to its diameter of approximately 15-20 μm (note, that cell rotation without its translational movement does not affect CRRC measurements). In our case, the time interval between the frames was 3 min while, according to the available data (30), it would take days for the cells used here to move a distance of 15-20 μm in both monolayers and spheroids. A2780 cells belong to a class of slow-migrating OC cells (30); their migration is noticeable only in a time-scale of several days (30). It should be noted that cell mobility within the cell culture can vary greatly (31), and for some cell types, cells in a 2D culture have greater mobility than cells within a 3D culture (32,33).

To conclude, this work demonstrates unique capabilities of CRRC in studying heterogeneity of cell population with respect to MDR activity. This study answers the question of whether cell clustering can influence (in principle) intrinsic and acquired MDR differently; the answer is 'yes'. This study is, of course, limited to one cell line; answering this question for other cell lines will require further investigation. It is important to emphasize that this study did not aim to answer any other question. In particular, consequences of spheroidal MDR activation for cell proliferation and survival were beyond the scope of this work for two reasons. First, they are well documented, for example, in the studies related to cell-adhesion-mediated drug resistance (34). Second, these consequences are commonly studied in the cell-population format, and conclusions that can be obtained from such studies cannot contribute significantly to conclusions made from the CRRC study performed in the single-cell format. Further, our data show that the extent of MDR-transport activation in OC cell clusters strongly depends on the previous chemotherapeutic history of spheroid-forming A2780 cells. This fact, if confirmed in primary ovarian tumor cells, will help clinicians

to optimize OC treatment, since therapeutic approaches might have different outcomes for drug-naïve and drug-exposed tumors. If the observed phenomena are found in other types of cancer cells, the last conclusion can be extended to those types of cancer.

Acknowledgements

The authors thank Dr Sven Kochmann (Centre for Research on Biomolecular Interactions, York University, Toronto, Canada) for technical help.

Funding

This research was funded by the Natural Sciences and Engineering Research Council of Canada (grant no. 238990).

Availability of data and materials

All data generated or analyzed during this study are included in this published article or available as supplementary materials on: https://doi.org/10.6084/m9.figshare.13003268.v2.

Authors' contributions

VK, CP, LEA, GL, AC and SNK conceptualized the current study. VK and SNK developed the methodology. VK and MBDO performed the experiments. VK, MBDO and SNK analyzed the data. VK and MBDO confirm the authenticity of all the raw data. VK drafted the manuscript. writing-review and editing, CP, LEA, GL, AC and SNK wrote, reviewed and edited the manuscript. supervision, SNK supervised, provided administrative support and acquired funding for the current study. All authors have read and agreed to the published version of the manuscript.

Ethics approval and consent to participate

Not applicable.

Patient consent for publication

Not applicable.

Competing interests

The authors declare that they have no competing interests.

References

1. Rueff J and Rodrigues AS: Cancer drug resistance: A brief overview from a genetic viewpoint. Methods Mol Biol 1395: 1-18, 2016.
2. Norouzi-Barough L, Sarookhani MR, Sharifi M, Moghbelinejad S, Jangjoo S and Salehi R: Molecular mechanisms of drug resistance in ovarian cancer. J Cell Physiol 233: 4546-4562, 2018.
3. Srivastava R, Srivastava A and Chochung Y: Multidrug resistance in cancer (review). Int J Oncol 9: 879-884, 1996.
4. Zhang Y, Sriraman S, Kenny H, Luther E, Torchilin V and Lengyel E: Reversal of chemoresistance in ovarian cancer by co-delivery of a P-glycoprotein inhibitor and paclitaxel in a liposomal platform. Mol Cancer Ther 15: 2282-2293, 2016.
5. Hwang WL, Hwang KL and Miyamoto DT: The promise of circulating tumor cells for precision cancer therapy. Biomark Med 10: 1269-1285, 2016.
6. Guiliano M, Shaikh A, Lo HC, Arpino G, De Placido S, Zhang XH, Cristofanilli M, Shiff R and Trivedi MV: Perspective on circulating tumor cell clusters: Why it takes a village to metastasize. Mol Cancer Res 78: 845-852, 2018.
7. Lee M, Kim EJ, Cho Y, Kim S, Chung HH, Park NH and Song YS: Predictive value of circulating tumor cells (CTCs) captured by microfluidic device in patients with epithelial ovarian cancer. Gynecol Oncol 145: 361-365, 2017.
8. Koshkin V, Kochmann S, Sorupanathan A, Peng C, Ailles LE, Liu G and Krylov SN: Cytometry of reaction rate constant: Measuring reaction rate constant in individual cells to facilitate robust and accurate analysis of cell-population heterogeneity. Anal Chem 91: 4186-4194, 2019.
9. Koshkin V, Bleker de Oliveira M, Peng C, Ailles LE, Liu G, Covens A and Krylov SN: Spheroid-based approach to assess the tissue relevance of analysis of dispersed-settled tissue cells by cytometry of the reaction rate constant. Anal Chem 92: 9348-9355, 2020.
10. Durand RE: Flow cytometry studies of intracellular adriamycin in multicell spheroids in vitro. Cancer Res 41: 3495-3498, 1981.
11. Xu G, Zhong Y, Munir S, Yang BB, Tsang BK and Peng C: Nodal induces apoptosis and inhibits proliferation in human epithelial ovarian cancer cells via activin receptor-like kinase 7. J Clin Endocrinol Metab 89: 5523-5534, 2004.
12. Sasaki H, Sheng Y, Kotsuji F and Tsang BK: Down-regulation of X-linked inhibitor of apoptosis protein induces apoptosis in chemoresistant human ovarian cancer cells. Cancer Res 60: 5659-5666, 2000.
13. Jendželovská Z, Jendželovský R, Hiľovská L, Kovaľ J, Mikeš J and Fedoročko P: Single pre-treatment with hypericin, a St. John's wort secondary metabolite, attenuates cisplatin- and mitoxantrone-induced cell death in A2780, A2780cis and HL-60 cells. Toxicol In Vitro 28: 1259-1273, 2014.
14. Raghavan S, Ward MR, Rowley KR, Wold RM, Takayama S, Buckanovich RJ and Mehta G: Formation of stable small cell number three-dimensional ovarian cancer spheroids using hanging drop arrays for preclinical drug sensitivity assays. Gynecol Oncol 138: 181-189, 2015.
15. Ween MP, Armstrong MA, Oehler MK and Ricciardelli C: The role of ABC transporters in ovarian cancer progression and chemoresistance. Crit Rev Oncol Hematol 96: 220-256, 2015.
16. Cunnea P and Stronach EA: Modeling platinum sensitive and resistant high-grade serous ovarian cancer: Development and applications of experimental systems. Front Oncol 4: 81, 2014.
17. Li N, Zuo H, Chen L, Liu H, Zhou J, Yao Y, Xu B, Gong H, Weng Y, Hu Q, *et al*: Circfulating tumor cell detection in epithelial ovarian cancer using dual-component antibodies targeting EpCAM and FRα. Cancer Manag Res 11: 109939-10948, 2019.
18. Mahdizadeh S, Karimi G, Behravan J, Arabzadeh S, Lage H and Kalalinia F: Crocin suppresses multidrug resistance in MRP overexpressing ovarian cancer cell line. Daru 24: 17, 2016.
19. Friedrich J, Seidel C, Ebner R and Kunz-Schughart LA: Spheroid-based drug screen: Considerations and practical approach. Nat Protoc 4: 309-324, 2009.
20. Frankel A, Buckman R and Kerbel RS: Abrogation of taxol-induced G2-M arrest and apoptosis in human ovarian cancer cells grown as multicellular tumor spheroids. Cancer Res 57: 2388-2393, 1997.
21. Acker H, Carlsson J, Holtermann G, Nederman T and Nylén T: Influence of glucose and buffer capacity in the culture medium on growth and pH in spheroids of human thyroid carcinoma and human glioma origin. Cancer Res 47: 3504-3508, 1987.
22. Morrow CS, Peklak-Scott C, Bishwokarma B, Kute TE, Smitherman PK and Townsend AJ: Multidrug resistance protein 1 (MRP1, ABCC1) mediates resistance to mitoxantrone via glutathione-dependent drug efflux. Mol Pharmacol 69: 1499-1505, 2006.
23. Nakano A, Tsuji D, Miki H, Cui Q, El Sayed SM, Ikegame A, Oda A, Amou H, Nakamura S, Harada T, *et al*: Glycolysis inhibition inactivates ABC transporters to restore drug sensitivity in malignant cells. PLoS One 6: e27222, 2011.
24. Teng YN, Hsieh YW, Hung CC and Lin HY: Demethoxycurcumin modulates human P-glycoprotein function via uncompetitive inhibition of ATPase hydrolysis activity. J Agric Food Chem 63: 847-855, 2015.

25. Ham SL, Joshi R, Thakuri PS and Tavana H: Liquid-based three-dimensional tumor models for cancer research and drug discovery. Exp Biol Med (Maywood) 241: 939-954, 2016.
26. Szakács G, Annereau JP, Lababidi S, Shankawaram U, Arciello A, Bussey KJ, Reinhold W, Guo Y, Kruh GD, Reimers M, *et al*: Predicting drug sensitivity and resistance: Profiling ABC transporter genes in cancer cells. Cancer Cell 6: 129-137, 2004.
27. Howard GR, Johnson KE, Rodriguez Ayala A, Yankeelov TE and Brock A: A multi-state model of chemoresistance to characterize phenotypic dynamics in breast cancer. Sci Rep 8: 12058, 2018.
28. Sun FF, Hu YH, Xiong LP, Tu XY, Zhao JH, Chen SS, Song J and Ye XQ: Enhanced expression of stem cell markers and drug resistance in sphere-forming non-small cell lung cancer cells. Int J Clin Exp Pathol 8: 6287-6300, 2015.
29. He M, Wu H, Jiang Q, Liu Y, Han Li, Yan Y, Wei B, Liu F, Deng X, Chen H, *et al*: Hypoxia-inducible factor-2α directly promotes BCRP expression and mediates the resistance of ovarian cancer stem cells to adriamycin. Mol Oncol 13: 403-421, 2019.
30. Hallas-Potts A, Dawson JC and Herrington CS: Ovarian cancer cell lines derived from non-serous carcinomas migrate and invade more aggressively than those derived from high-grade serous carcinomas. Sci Rep 9: 5515, 2019.
31. Partin AW, Schoeniger JS, Mohler JL and Coffey DS: Fourier analysis of cell motility: Correlation of motility with metastatic potential. Proc Natl Acad Sci USA 86: 1254-1258, 1989.
32. Galarza S, Kim H, Atay N, Peyton SR and Munson JM: 2D or 3D? How cell motility measurements are conserved across dimensions in vitro and translate in vivo. Bioeng Transl Med 5: e10148, 2019.
33. Luzhansky ID, Schwartz AD, Cohen JD, MacMunn JP, Barney LE, Jansen LE and Peyton SR: Anomalously diffusing and persistently migrating cells in 2 and 3D culture environments. APL Bioeng 2: 026112, 2018.
34. Raghavan S, Mehta P, Horst EN, Ward MR, Rowley KR and Mehta G: Comparative analysis of tumor spheroid generation techniques for differential in vitro drug toxicity. Oncotarget 7: 16948-16961, 2016.